Conjugate Heat Transfer in Diverging Microchannels

A thesis submitted in partial fulfillment of the

Requirements for the degree of

Bachelor of Technology

in

Mechanical Engineering

by

V Rajesh Kumar

(111ME0308)

Department of Mechanical Engineering

National Institute of Technology Rourkela

Rourkela 769008 (Odisha)

CERTIFICATE

This is to certify that the thesis entitled "**CONJUGATE HEAT TRANSFER IN DIVERGING MICROCHANNELS**" submitted to the National Institute of Technology, Rourkela by **V Rajesh Kumar (111ME0308)** for the award of the Degree of Bachelor of Technology in Mechanical Engineering is a record of bona fide research work carried out by him under my supervision and guidance. The results presented in this thesis has not been, to the best of my knowledge, submitted to any other University or Institute for the award of any degree or diploma. The thesis, in my opinion, has reached the standards fulfilling the requirement for the award of the degree of Bachelor of technology in accordance with regulations of the Institute.

Dr. Manoj Kumar Moharana
Assistant Professor
Department of Mechanical Engineering
National Institute of Technology Rourkela

Date:

SELF-DECLARATION

I, Mr. V Rajesh Kumar, Roll No. 111ME0308, a student of B. Tech (2011-15) from the Department of Mechanical Engineering, National Institute of technology Rourkela do hereby declare that I have not implemented any kind of unfair and malicious means and carried out the research work ethically to the best of my knowledge. If implementation of any kind of unfair and malicious means is found in this thesis work at a later stage, then appropriate action can be taken against me including withdrawal of this thesis work and even withdrawal of degree in extreme circumstances.

V. Rajesh Kumar

NIT Rourkela
28 May 2015

V Rajesh Kumar

ACKNOWLEDGEMENT

I have taken efforts in this project. However, it would not have been possible without the kind support and help of many individuals and the department. I would like to extend my sincere thanks to all of them.

I would like to express my gratitude and special thanks to my project guide Dr. Manoj Kumar Moharana, Assistant Professor, Department of Mechanical Engineering, NIT Rourkela, for all the cooperation and time.

My special thanks to all the students as well as Professors of thermal department for giving their whole hearted cooperation.

V Rajesh Kumar
(111ME0308)

ABSTRACT

A numerical study has been carried out to determine the effects of axial wall conduction during single-phase steady laminar flow of fluid through rectangular diverging (across the length of the channel) cross-sectional microchannel involving conjugate heat transfer. A constant heat flux boundary condition has been applied on the bottom surface of the substrate on which the microchannel is carved, while all other surfaces of the substrate are subjected to adiabatic condition to simulate insulation. The simulations have been carried out by varying wall thickness to channel height ratio (δ_{sf} ~1-24), solid substrate conductivity to working fluid conductivity ratio (k_{sf} ~0.17-703) and Reynolds number (Re~100-1000). For the purpose of comparison simulations for uniform cross-sectional area across the microchannel length has also been carried out. Four different geometrical dimensions, eleven substrate materials and three Reynolds numbers have been considered in this study, which would cover the common scope of uses experienced in microfluids/microscale heat transfer areas and would provide a wide parametric variation for a generalized visualization of the outcome of this study. The results demonstrate that the conductivity ratio is the pivotal parameter in affecting the extent of axial wall conduction. Very low and very high values of k_{sf} would result in decrease of Nusselt number. Such a sensation also exists for uniform square and circular cross-sections.

Keywords: microchannel, axial wall conduction, conjugate heat transfer, Nusselt number

CONTENTS

LIST OF TABLES:

LIST OF FIGURES:

NOMENCLATURE

A	cross-sectional area (m^2)
A_{sf}	cross-sectional area ratio (A_s /A_f)
Bi	Biot Number (-)
C_p	specific heat (J/kg K)
d	diameter of circular tube (m)
D_h	hydraulic diameter (mm)
DA	diverging cross-sectional microchannel
h_z	local heat transfer coefficient (W/m^2 K)
k	thermal conductivity (W/m K)
k_{sf}	wall to fluid thermal conductivity ratio (k_s/k_f)
L	channel length (mm)
M	axial conduction number (-)
$\dot{m}$	mass flow rate (kg/s)
NTU	number of transfer units (-)
Nu	Nusselt number ($h.D_h/k_f$)
P	parameter for axial conduction (-)
Pe	Peclet number (Re.Pr)
Pr	Prandtl number ($c_p.\mu/k_f$)
Q'	heat flux applied at the bottom surface of the substrate (W/m^2)
q'	experienced average heat flux at the channel walls (W/m^2)
q'_z	average local heat flux at any axial location (W/m^2)
r	radius (m)
Re	Reynolds number ($\rho.u .D_h /\mu$)
T	temperature (K)
UA	uniform cross-sectional microchannel
u	average velocity of fluid in the channel (m/s^2)
z	axial distance along the channel length (mm)
z*	non-dimensional axial distance along the channel length (-)

Greek Symbols:

δ	thickness (mm)
δ_{sf}	ratio of substrate thickness to channel height (δ_s/δ_f)
ΔT	temperature difference between inlet and outlet location (K)
Θ	non-dimensional temperature (-)
λ	conduction parameter (-)
μ	dynamic viscosity (Pa.s)
ξ	length ratio (-)
ρ	density (kg/m^3)
φ	non-dimensional heat flux (-)
ω	width of the solid substrate (mm)
ω_1	width of the liquid substrate at inlet (mm)
ω_2	width of the liquid substrate at outlet (mm)

Subscripts:

cond	conductive
conv	convective
i	inlet condition, inner
o	outlet condition, outer
s	solid
w	wall surface
f	fluid
z	axial length along the channel

CHAPTER 1

INTRODUCTION

1.1 Background

From the time of domestication of fire, a lot of research was done in the area of heat transfer and transfer of heat from one location to other, from one medium to another while overcoming the challenges imposed by varied constraints were the objectives of work. In early 19^{th} and 20^{th} centuries, research focus was on increasing the surface area to facilitate higher heat transfer rates. Shell and tube heat exchangers prevailed mostly during those days due to their ability to increase the size to individual units and in some cases, rivalling the sizes of modest single-family homes. Then, heat exchangers had set its market because of high demand from aircraft, submarine, spacecraft, automotive and transportation sectors. Considering applications of gas, plate-fin exchangers using small size passages were developed. Novel fins, especially micro fins applications became dominant in single phase and two phase applications and also twisted tapes and enhanced devices were widely used to facilitate a major uplift in old generation technology with the utilization of big hydraulic diameters. The market sector adopted the flexibility of heat exchangers. By using compact generators of sub-millimetre sized flow passages, cryogenic industry is ahead by utilizing the effectiveness of heat exchangers. On considering the benefits of using micro-fin tubes, refrigeration industry has adopted it in evaporators and condensers. Single phase and two phase applications became popular throughout the heat transfer industry. This started the era of microchannels.

Microchannels are the channels used for enhanced species transport whose dimensions are in the range of few micrometers to about 1000 μm. For a channel to be called as microchannel the characteristic length (hydraulic diameter) of the channel should be comparable with wall thickness. The most recent decade has seen quick advance in the advancement of microchannel based thermo-fluidic frameworks. Improved species transport in such micro geometries is the prime inspiration for their improvement. It is likewise watched that the general measurements of the cross section of the substrate or the microchannel (for illustration, the divider thickness, the inter channel pitch, the substrate thickness etc.) generally scales with the hydraulic diameter of the channel or pipe used for the flow purpose.

1.2 Application areas

Because of higher thermal performance of minichannels, they are increasingly being employed in a lot of process applications. In the automobile and space industries, minichannels proved important in solving the serious space requirement problems. Compact heat exchangers adopt minichannels in these as well as many other areas. The microelectronics scientists found that the microchannel range is the required compromise in microelectronics especially in cooling applications. In biomedical and optics areas microchannels as well as nanochannels are often used. Mechanical engineers are presently doing rigorous research in this field to fully study the trends of microchannels to apply them in different areas.

1.3 Complications

In case of normal channels the hydraulic diameter is very large in comparison to wall thickness. So in conventional channels, the effect of axial wall conduction is very minimal and hence valid results can be obtained by neglecting this effect. But in case of microchannels, this effect cannot be neglected as wall thicknesses are comparable with the hydraulic diameter. In the design analysis stage, if this effect is overlooked, would lead to erroneous results and inconsistencies in data interpretation. In this scenario there is a conversion of a normal problem of pure convective heat transfer type into a problem of multi-mode heat transfer i.e., convection as well as conduction in walls. The heat flux and the temperature distribution of the microchannel depends on different parameters including the dimensions of the domains and the thermal properties of solid and fluid involved. The resulting conjugate nature of heat transfer results in severe distortion of the thermal boundary layer at the fluid-solid wall interface especially in the large temperature gradient regions, like, in the thermal entrance region of the channel.

1.4 Motivation

In case of flow in microchannels, conjugate heat transfer is leading to strong multidimensional coupling. The lengths in the transverse directions are comparable to the wall thickness or substrate thickness. As the transverse dimensions decrease, overall hydraulic diameter becomes comparable to that of transverse dimensions, which would in turn further lead to stronger influence of this coupling. Thus, it is important to explicitly identify the parameters affecting this phenomenon. Identifying these parameters would lead us to the situation where we would be able to select these parameters, thus optimizing the situation.

A lot of numerical and experimental studies regarding conjugate heat transfer in microchannels are available but most of them deal with uniform cross-sectional microchannels. Also, studies involving parametric variation are few. But, rectangular microchannels are becoming more and more important because of its extensive use in heat exchanger equipment and applications. To suffice these applications wide varieties of materials are used along with different flow conditions. Also different substrate dimensions are chosen according to the need. For evaluating the realistic heat transfer coefficients under such wide range of design estimates, thorough parametric variation study is needed. The prime motive of this study is to address these issues in detail.

CHAPTER 2

LITERATURE REVIEW

Axial back conduction is not a very new conceptual development. It is by now a well-established concept. It is not only restricted to microchannels. Peterson [1] had detailed the effect of axial wall conduction in normal size conventional heat exchangers. Bahnke and Howard [2] had also dealt with axial back conduction for analyzing recuperators. For the purpose of analysis of internal single-phase convection flows, "conduction parameter", has been introduced in the literature, which gives the relative importance of conduction as compared to the flow of energy carried by a fluid. It is quantified as the ratio of axial heat transfer to the energy carried by the fluid in axial direction with in the solid channel/duct. This parameter was first used by Bahnke and Howard [2] and then by Peterson [1]

$$\lambda = k_s . A_s / m.\mathbf{c_p}.\mathrm{L} \tag{1}$$

Davis and Gill [3] have found that the Peclet number of fluids is smaller as compared to that of solids. So, they stated that axial conduction in fluids can be neglected and only the axial conduction in the wall i.e., through solid domain has to be taken care of.

A lot of studies have been done on microscale heat transfer, especially on axial wall conduction. So, there exists a parameter called axial wall conduction, P in the literature. This parameter is defined differently by different authors. Petukhov [4], Faghri and Sparrow [5], Cotton and Jackson [6] and Chiou et al. [7] have defined P as follows respectively.

$$P = k_{sf}\left[1-\left(1+\left(\delta / r_i\right)\right)^2\right] \tag{2}$$

$$P = k_{sf}\left(\delta / r_i\right) \tag{3}$$

$$P = k_{sf}\left[\frac{\delta}{d_i}\left(1+\frac{\delta}{\delta_i}\right)\right]\left(\frac{1}{Pe^2}\right) \tag{4}$$

$$P = k_{sf} . A_{sf} . \left(\frac{d_i}{L}\right)\left(\frac{1}{Pe}\right) \tag{5}$$

To understand the effect of axial heat conduction in a mini/micro counter flow heat exchanger, Maranzana et al. [8] has carried out analytical study as well as numerical simulation. Taking into account their investigation, they proposed that the impact of axial wall conduction in the substrate on the heat transfer coefficient can be ignored, if $M<10^{-2}$. Both the conduction parameter (k) and the axial conduction number (M). They have come to this conclusion based on the assumption that difference of axial wall temperatures and fluid domain temperatures between inlet and outlet being same. This assumption is not realistic. They used the following formulae for evaluating value of M.

$$NTU = \frac{h.L}{\rho_f . \mathrm{c}_{p-f} . \delta_f . u} \tag{6}$$

$$Bi = \frac{h.\delta_s}{k_s} \tag{7}$$

$$\xi = \frac{\delta_s}{L} \tag{8}$$

Zhang et al. [9] by taking the effect of individual temperature differences between the inlet and outlet location in the solid wall as well as in fluid domain, proposed the conduction number, as revised by Li et al. [10] , which is given by

$$M = \frac{q'_{cond}}{q'_{\mathrm{conv}}} = \left(\mathrm{k}_s \frac{(\delta_s . \omega)/L}{(\rho_f . \mathrm{c}_{p-f} . \delta_f . \omega . u)} \right) \tag{9}$$

Toh et al. [11] had explored the heat transfer and fluid flow phenomena inside a three dimensional pre-heated microchannel. They solved the steady, laminar and heat transfer equations utilizing a finite-volume technique. The numerical technique is accepted with accessible experimental data. They found that at lower Reynolds numbers the temperature of the water increases, prompting an abatement in the viscosity and henceforth little frictional losses.

To understand the heat transfer behavior of water flowing through triangular silicon micro-channels, Tiselj et al. [12] carried both the experimental as well as numerical analysis. Their study showed that the bulk fluid and wall temperature doesn't vary linearly along the channel length.

An experimental investigation of single-phase laminar flow in circular micro-ducts of different diameters have been done by Celata et al. [13] and through their results they showed that Nusselt number decreases as diameter decreases. The thermal entrance effects have also been investigated. The dependence of the Nusselt number also on Reynolds number is found.

Tuckerman and Pease [14] has introduced the concept of micro channel heat sinks and illustrated demonstrations to show that chips can be cooled by using forced convection of water through microchannels. A rectangular micro-channel having a channel dimensions 50 microns of width and 302 microns of depth was fabricated in a wafer made of silicon. It had a capacity to dissipate 790 W/cm^2 and without undergoing any phase change the temperature of substrate could rise as high as 710^oC above temperature of water inlet. This was a giant step in the field of microchannels.

Moharana et al. [15] had conducted both experimental and numerical analysis of axial wall conduction in single-phase simultaneously developing flow in a rectangular mini-channel array. They demonstrated that at higher value of the axial conduction number (M), the conjugate effects dominate due to the presence of axial back conduction in the substrate. This results in the decrease of local Nusselt numbers as compared to that evaluated in numerical model.

Moharana et al. [16] numerically studied axial wall conduction in a square microchannel and considered wide parametric variation of conductivity ratio, substrate thickness and flow Re. The bottom wall being given a constant heat flux with all other walls being insulated. The study showed that thermal conductivity ratio of solid domain and fluid domain is the key factor in determining the effect of axial wall conduction. There exists an optimum conductivity ratio at which average Nusselt number gets maximized. Very high conductivity ratio would increase the axial conduction and very low value makes the situation similar to that of one side wall heating and thus decreasing the average Nusselt number.

Moharana and Khandekar [17] numerically studied the effect of aspect ratio on the performance of microchannels. They considered a fixed substrate size and varied the aspect ratio (0.45-4.0) at different conditions, namely, constant cross-sectional area, constant heated perimeter, constant height and constant width. They demonstrated that depending on the condition, at constant flow and thermal conductivity there exists a minima in average Nusselt number at around an aspect ratio of 2. They also recommended that it is better to use aspect ratios greater

than 2 owing to the difficulty in manufacturing and lesser slope of increase in average Nusselt number in case of aspect ratios lesser than 2.

Moharana and Khandekar [18] had studied the influence of axial wall conduction in microtubes at two different conditions, namely, constant heat flux and constant wall temperature. A wide parametric variation is done by varying conductivity ratios, Reynolds number and thickness of the tube. They proposed that conductivity ratio is the pivotal parameter. There exists an optimum average Nusselt for a range of conductivity ratios in case of constant heat flux boundary condition but in case of constant wall temperature condition such optima does not exist, rather the average Nusselt number increases with decreasing conductivity ratio. Also, they stated that higher wall thicknesses will increase the average Nusselt number.

Moharana and Mishra [19] through their numerical study found that conductivity ratio is major parameter affecting the influence of axial wall conduction in pulsating single phase laminar flow. They mainly demonstrated that there is an optimisation of Nusselt number for a particular pulsating frequency while keeping all other parameters constant.

Moharana et al. [20] through their parametric study demonstrated that to correctly estimate the local Nusselt number in case of developing flow in microchannels depending on geometry of models, flow conditions and thermo-physical properties, conjugate heat transfer effects must be considered.

Kumar and Moharana [21] had conducted numerical study to determine the effect of axial wall conduction in partially heated microtubes. They had considered a wide parametric variation by varying conductivity ratios, thickness and Reynolds number. They considered a microchannel with some part near inlet and outlet sections being kept insulated and the remaining part being imposed a constant wall temperature condition. They mainly proposed that average Nusselt number increases with decreasing wall conductivity and increases for thicker walls.

Yadav et al. [22] numerically studied the effect of axial wall conduction in microtubes at low temperature. A wide parametric variation is considered in this study by taking Helium. They showed that conductivity ratio and wall thickness are the pivotal parameters. They demonstrated that there is an existence of a conductivity ratio for which the average Nusselt number is optimized. Average Nusselt number gets low at higher wall thicknesses and gets increased as flow value of Helium increases.

CHAPTER 3

METHODOLOGY

3.1 Identification of the parameters and its range:

In every heat transfer problem there exists a lot of parameters which would affect the final solutions and conclusions. But, only some of them play dominant roles in the results obtained. Similarly, in this present problem there are many parameters which may affect the conjugate nature of the heat transfer. Thermal conductivity of solid, thermal conductivity of liquid, wall thicknesses, velocity of flow and heat capacities are some of them to be mentioned. Identifying the influencing parameters and to decide the range of their variation is the initial task.

The phenomenon of conduction is more dominant in solids as compared to fluids like water and air, owing to their low Peclet number. Peclet number of a material is defined as the ratio of conduction heat transfer to convection heat transfer in a material. So, we can comfortably neglect the axial back conduction in fluid domain and hence, the thermal conductivity of fluid domain. As the effect of axial wall conduction is the matter of interest, thermal conductivity of only the solid domain would play an important role in this problem. The dynamic parameters like mass flow rate and velocity would also possibly play a vital role. Most of these dynamic parameters have direct relationship with Reynolds number. So, by taking Reynolds number as an influencing parameter will cover all these dynamic parameters. As the distance at which heat flux is applied from the fluid domain increases, the distortion of boundary condition increases. So, solid wall thickness is also an important parameter.

In this present scenario of application of microchannels and microfluids, microchannels with a wide range of thermal conductivities are used. So, in order to cover this wide range, materials with k_s values with their corresponding k_{sf} (= k_s/k_f) values, mentioned in Table1 have been taken for consideration. Also, the fluid domain is kept constant by taking water as the fluid domain material. Since, fluid domain play a very less significant role, only δ_s (depth of the bottom solid wall) is varied by keeping δ_f (depth of fluid domain) constant. Generally, in microchannel applications, Reynolds number over the range of 100 to 1000 are most common. So, the study has been done by taking three different Reynolds numbers. Table 2 would summarize all the parametric variations considered in this present study.

Table 1 : Material list

Material	**ρ (kg/m^3)**	**C_p (J/kgK)**	**k_s (W/mK)**	**k_f (W/mK)**	**k_{sf} (k_s/k_f)**
Sulfur	2070	708	0.206	0.61032	0.338
Silicon dioxide	2220	745	1.38	0.61032	2.261
Bismuth	9780	122	7.86	0.61032	12.88
Nicrome	8400	420	12	0.61032	19.66
SS 316	8238	468	13.4	0.61032	21.96
Constantan	8920	384	23	0.61032	37.69
Chromium steel	7822	444	37.7	0.61032	61.77
Bronze	8780	355	54	0.61032	88.48
Zink	7140	389	116	0.61032	190.1
Alloy 195	2790	883	168	0.61032	275.3
Silver	10500	235	429	0.61032	702.9

Table 2 : Parametric variation

Parameter	**Values over which the parameter is varied**
k_{sf}	0.33, 2.26, 12.87, 19.66, 21.96, 37.68, 61.77, 88.47, 190.06, 275.3,702.9
δ_{sf}	1, 2, 16, 24
Re	100, 500, 1000

3.2 Representation of the models:

The microchannel geometries as shown in the Fig. 1 and Fig. 2 have been considered for analysis. The geometry shown in the Fig. 3 is used for the analysis of diverging microchannel. The other two geometries shown in Fig. 1 and Fig. 2 have been used for the analysis of uniform cross-sectional microchannels for the purpose of comparison of the results with that of diverging microchnnel. The cross section of the geometry shown in Fig. 1 and Fig. 2 matches with that of inlet and outlet cross-sections of diverging microchannel respectively.

Four different models of Fig. 1 have been considered by varying the δ_{sf}. The analysis of uniform cross-section microchannels have been done at only one δ_{sf} value. The exact dimensions of the models have been taken as mentioned in the Table 3.

Table 3 : Dimensions of the models

Sl. No.	**Dimension**	**Value (in mm)**
1	L	60
2	ω	0.6
3	ω_1	0.2
4	ω_2	0.3
5	δ	0.4
6	δ_s	0.2, 0.4, 3.2, 4.8
7	δ_f	0.2

Since, all the geometries considered are symmetric in nature, only half the domains of the models shown in Fig. 4 are modelled using commercially available Ansys Fluent®.

During meshing an element size of 0.01 mm in X and Y directions and an element size of 0.3 mm in z direction is considered in the simulation based on the outcome of the grid independence test.

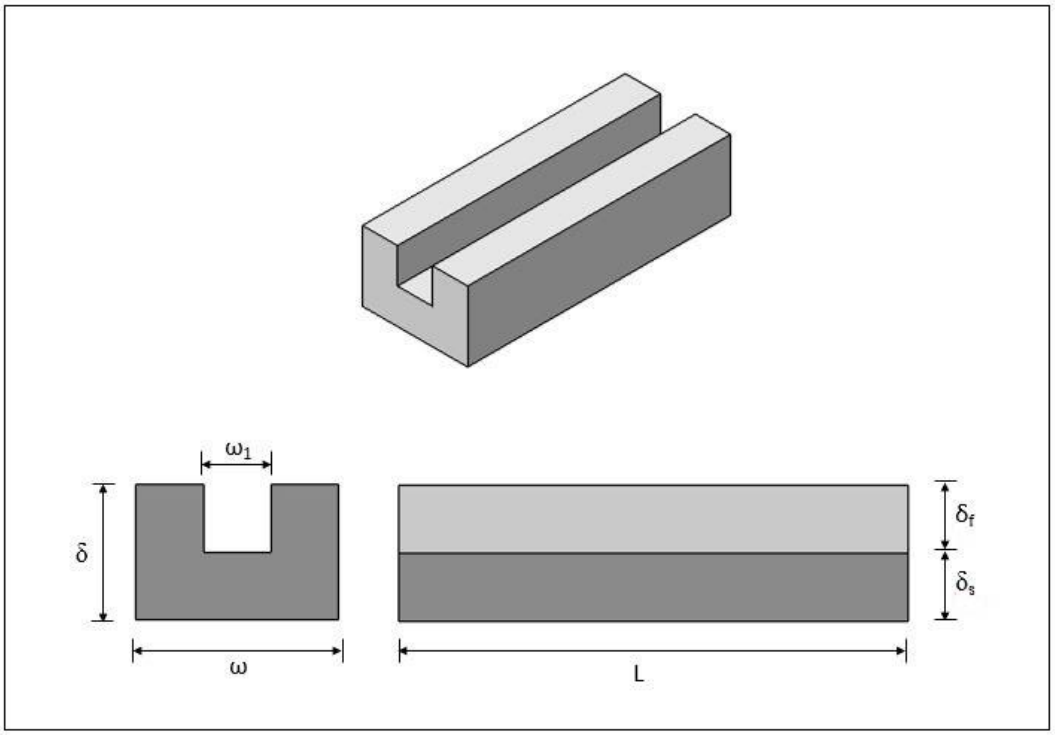

Figure 1 : Details of simulated domain of uniform cross-sectional microchannel whose cross-section matches with that of inlet of diverging microchannel

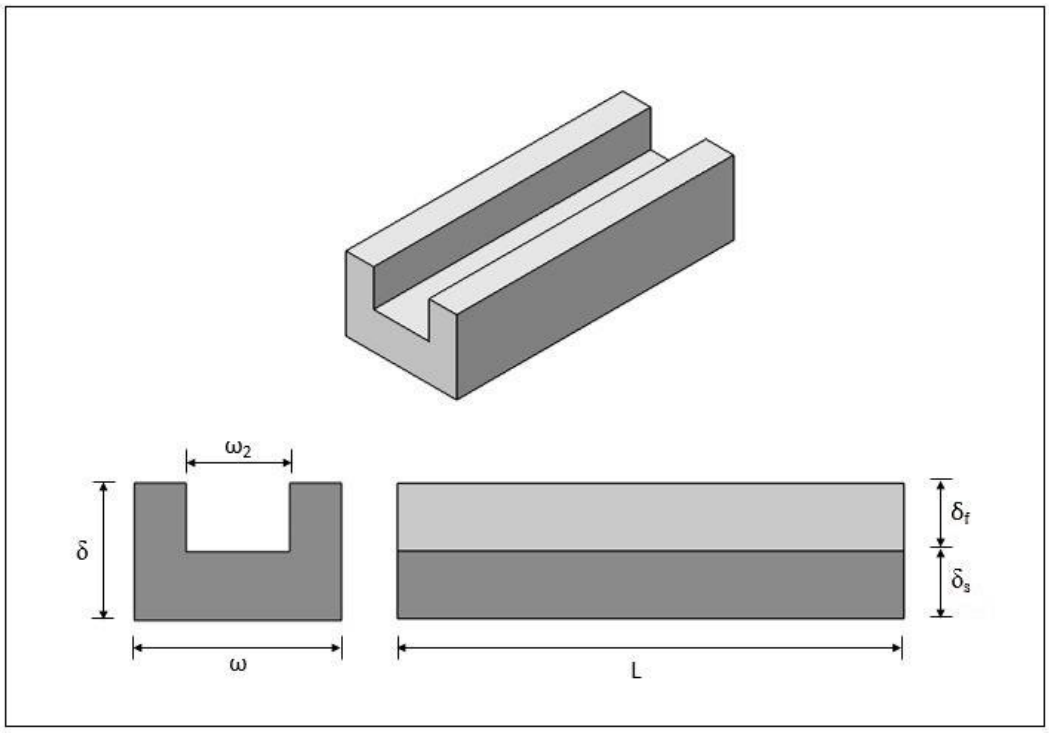

Figure 2: Details of simulated domain of uniform cross-sectional microchannel whose cross-section matches with that of outlet of diverging microchannel

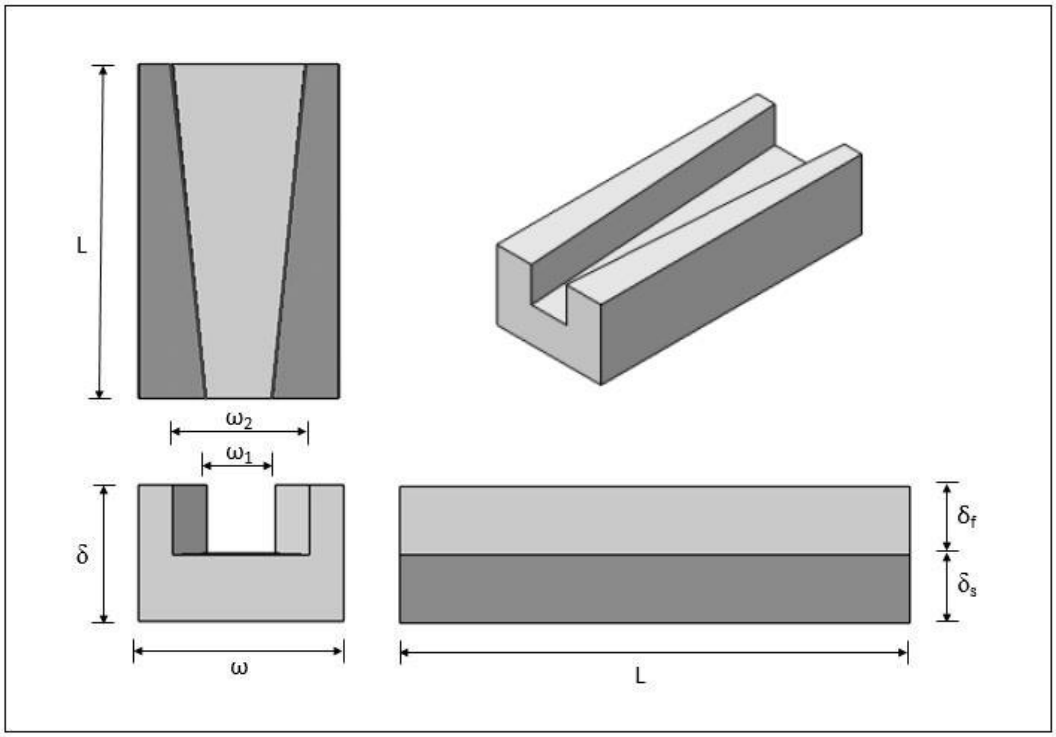

Figure 3: Details of simulated domain of diverging microchannel

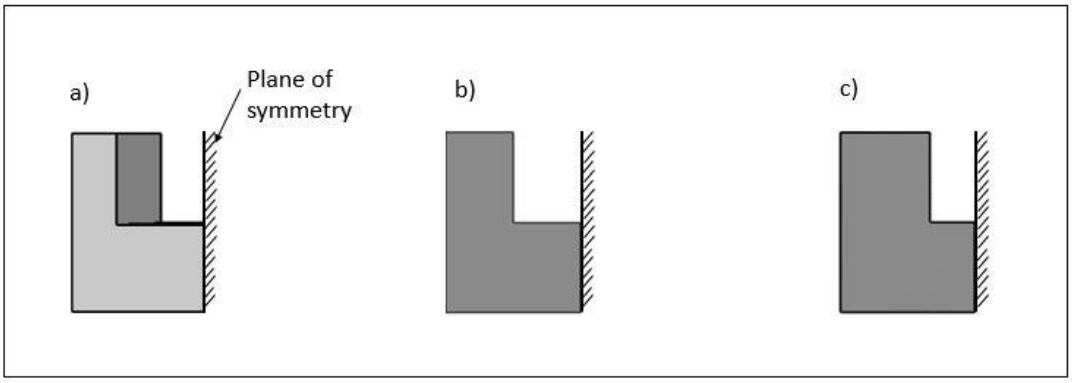

Figure 4: Half domains with symmetric planes a) Diverging microchannel b) Microchannel w.r.t outlet section c) Microchannel w.r.t inlet section

Table 4 : Mesh sizes of diverging microchannel substrate investigated

Sl no	ω/2 (in mm)	δ_s (in mm)	L (in mm)	δ_{sf} (in mm)	Mesh (half domain)
1	0.3	0.2	60	1	30×40×200
2	0.3	0.4	60	2	30×60×200
3	0.3	3.2	60	16	30×340×200
4	0.3	4.8	60	24	30×500×200

3.3 Analysis:

3.3.1 Boundary conditions:

The inlet temperatures of the fluid is kept constant at 300K. Secondly, constant heat flux condition is imposed on the bottom wall such that maximum temperature rise of the fluid will be 50 K, and all other walls are kept insulated. Since, the inlet, the value of the heat flux applied at the bottom depends only on Reynolds number and the velocity of flow at the inlet also depends on Reynolds number at the channel inlet. These calculations of heat flux and velocity of flow are done using Eq. (10-12).

$$\mathrm{Re} = \frac{\rho v D}{\mu} \tag{10}$$

$$\dot{m} = \rho A v \tag{11}$$

$$\dot{m} c_p \Delta T = q'' A_b \tag{12}$$

Here, A represents the cross-sectional area of the inlet of the considered model and A_b represents the bottom wall's surface area on which heat flux is applied.

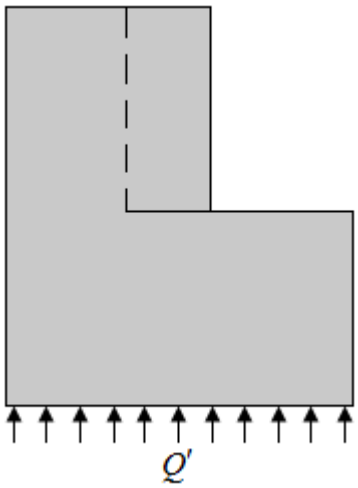

Figure 5: Domain shown with constant heat flux imposed on the bottom wall

Table 5 : Heat flux values for corresponding Reynolds numbers

Sl no.	Reynolds Number	Heat flux (in W/mm^2)
1	100	116515.17
2	500	582570.82
3	1000	1165142

3.3.2 Dimensionless parameters and data reduction:

For the purpose of data reduction, the following dimensionless variables have been used.

$$\phi = \frac{\overline{q_z}'}{\overline{q}'}, \quad \delta_{sf} = \frac{\delta_s}{\delta_f}, \quad z^* = \frac{z}{\mathrm{RePrD}_h}, \quad Nu_z = \frac{h_z \mathrm{D}_h}{k_f}, \tag{13}$$

$$\Theta = \frac{T - T_i}{T_o - T_i}, \qquad \Theta_f = \frac{T_{f|z} - T_{fi}}{T_{fo} - T_{fi}}, \qquad \Theta_w = \frac{T_{w|z} - T_{fi}}{T_{fo} - T_{fi}}$$

Here, z represents the axial distance starting from inlet section. $T_{w|z}$ and $T_{f|z}$ are the area weighted average of the wall temperature and mass weighted average of the fluid at a particular

z value. Q' represents the actual heat flux applied at the bottom and $\overline{q_z'}$ is the area weighted boundary average heat flux on the wall and $\bar{q}'$ is the heat flux value experienced at the conjugate solid-fluid boundary and it is calculated using following formula.

q' = Q' × (Area of the bottom wall/Total surface areas of conjugate walls) (14)

Also, the the average Nusselt number is calculated as follows.

$$\overline{Nu} = \int Nu_z dz \quad (15)$$

3.3.3 Grid independence test:

Grid independence test is an important test to be conducted before starting any analysis. Grid independence test is done on uniform cross-sectional microchannel. Nusselt number versus axial distance (i.e.; Nu vs z) plots have been plotted by taking different grid values. The local Nusselt number values in the fully developed region changes by 1% on an average on moving from the grid size of 23×31×150 to the grid size of 30×40×200 and it changes by below 1% on an average as we move from a grid size of 30×40×200 to 38×50×250. So, for all the cases the middle grid which would give an element size of 0.01 mm in x and y directions and 0.3 mm in z direction is taken. The grid independence plot has been shown in Fig. 6.

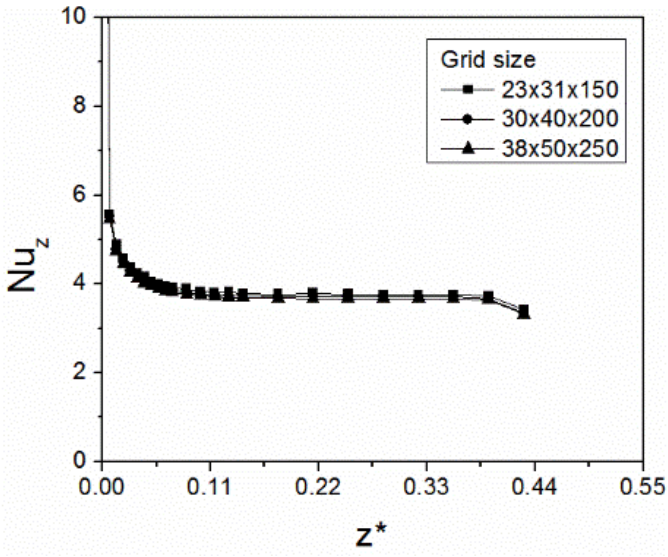

Figure 6: Local Nusselt number versus dimensionless axial distance at different grid sizes used to establish grid independence

3.3.4 Simulations:

The numerical analysis has been carried out using commercially available Ansys Fluent®. First, analysis of uniform cross sectional microchannels is done. Only, one δ_{sf} value is considered for both the cases. Two different Reynolds number and eleven different materials are used. So, 22 cases of simulations are done in each case. Then, the analysis of diverging channel is done by taking four different δ_{sf} values, eleven materials and three Reynolds numbers are used. So, 132 cases of simulations are done in this case.

For obtaining the wall fluxes, wall temperatures and bulk fluid temperatures, lines and planes are created on the conjugate walls (horizontal and vertical) and fluid domain respectively. Lines and planes are created with spacing of 1 mm from z = 0 to z = 10, 2 mm from z = 10 to 20 and 5 mm from z = 20 to 60. The initial spacing is taken smaller owing to the presence of developing region near the inlet. Wall temperatures are obtained by area-weighted averaging over the lines and fluid temperatures are obtained by mass weighted averaging over the planes. Using these values all the dimensionless parameters are calculated.

CHAPTER 4

RESULTS AND DISCUSSIONS

To know the parametric variation of heat flux, wall temperature, bulk fluid temperature and Nusselt number, plots of dimensionless heat flux, wall temperature, fluid temperature and Nusselt number with z* have been plotted. The parametric variation has been done by varying the values as shown in Table 2.

4.1 Observations:

4.1.1 Heat flux

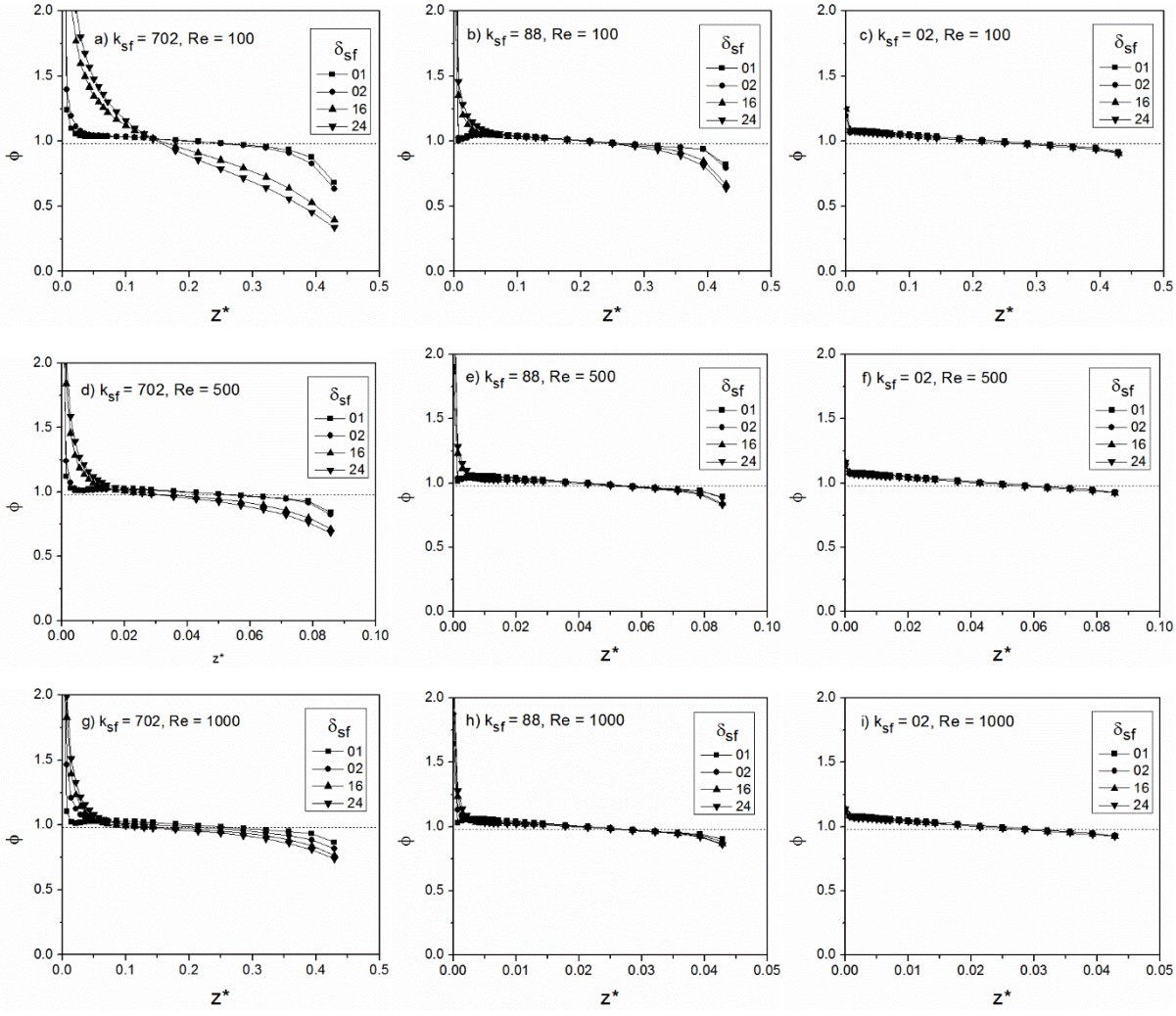

Figure 7: Axial variation of dimensionless heat flux of diverging microchannel

From the plots of dimensionless heat flux with z*, the following observations are made on the dependence of heat flux on k_{sf}, δ_{sf} and Re.

1. At lower k_{sf} values, the situation approaches ideal condition i.e., heat transfer experienced at the fluid-solid interface becomes equal to the applied flux (= 0.98 (in terms of dimensionless heat flux)). And the effect of variation of δ_{sf} is negligible.
2. At higher k_{sf} values, the values of the fluxes deviate considerably, especially, in the developing region. This is due to the decrease in the axial heat resistance due to the increase in the conductivity of the solid. As the axial resistance decreases, the axial back conduction increases and hence the heat flux values deviate from the ideal values.
3. As δ_{sf} increases, there is a shift in the actual boundary on which the constant heat flux is applied. So, because of this sensation, it is observed from the plots that, increase in δ_{sf} results in distortion in the heat flux values. This type of behavior is more dominant in case of higher k_{sf} values.

4.1.2 Dimensionless wall and fluid temperatures

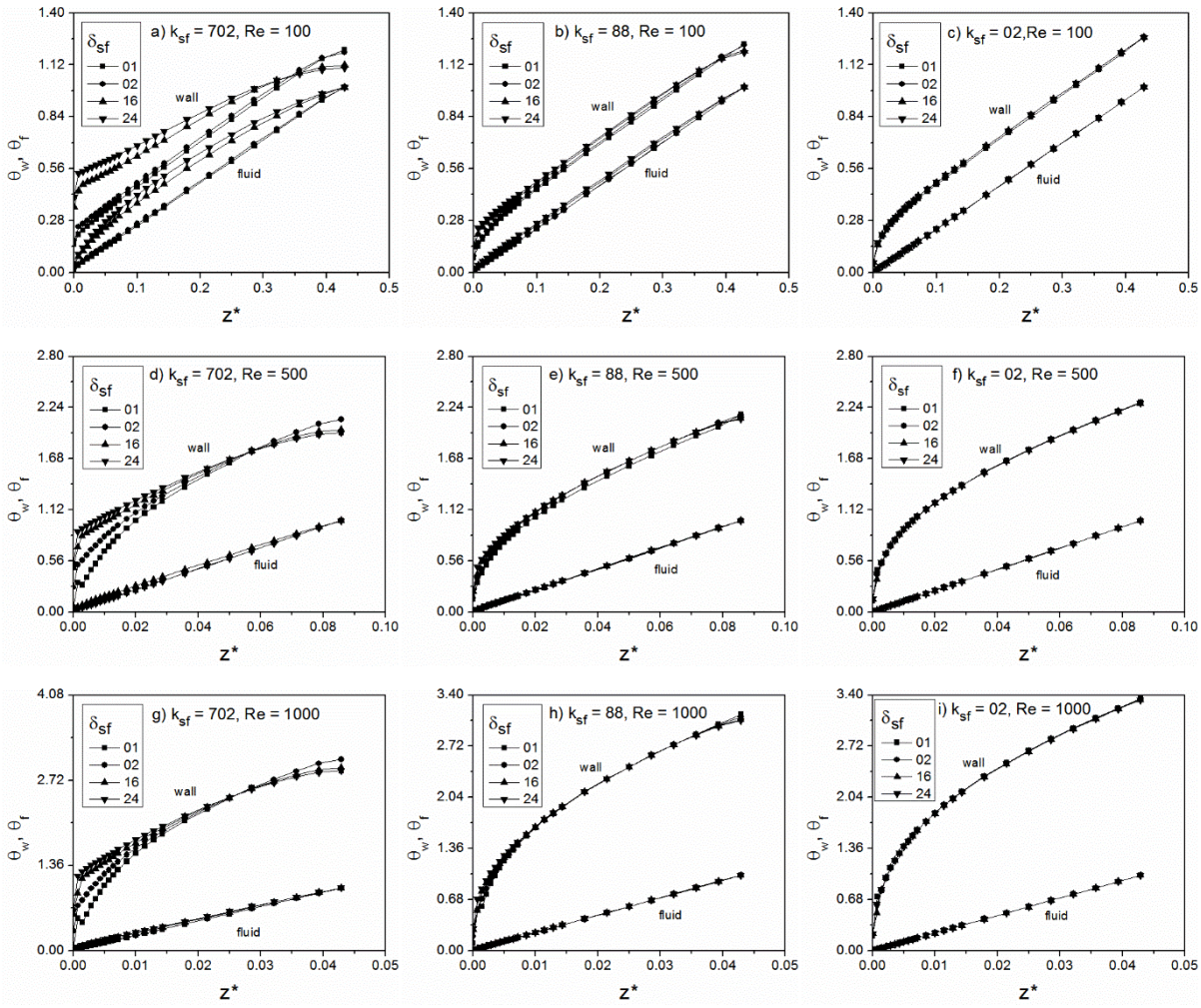

Figure 8: Axial variation of wall temperature and bulk fluid temperature of diverging microchannel

From the plots of dimensionless wall and fluid temperature with z*, following observations are made on the dependence of wall and fluid temperatures on k_{sf}, δ_{sf} and Re.

1. At low k_{sf} values, the ideal conventional theory applies which says that the difference between wall temperature and bulk temperature increases continuously within the thermal entrance length and remains constant thereafter. Also, after the thermal entrance length, the difference remains constant and the nature of the plots become linear.
2. At higher k_{sf} values, the situation explained above deviates. In case of higher k_{sf} values, there is a heat transfer from low stream to upstream invoking an isothermal boundary condition at the solid-fluid interface. As a result of this, the nature of the plots is no more linear, it becomes exponential in nature.
3. The situation deviates more and more from the ideal situation at higher δ_{sf} values as in the case of higher δ_{sf} values, the resistance of the bottom wall increases and there will be less conduction through the bottom wall, leading to more and more axial back conduction as more time will be available for the happening of axial back conduction.
4. It is also observed that as the Reynolds number increases, the difference between wall temperature and bulk fluid temperature increases.

4.1.3 Nusselt number

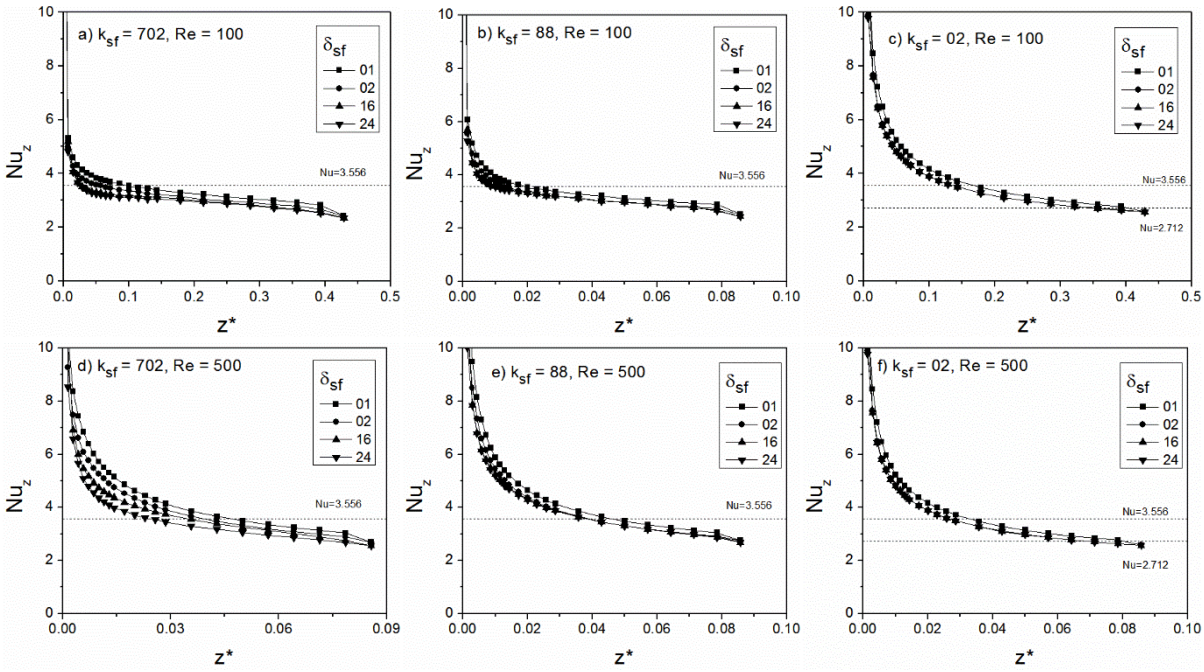

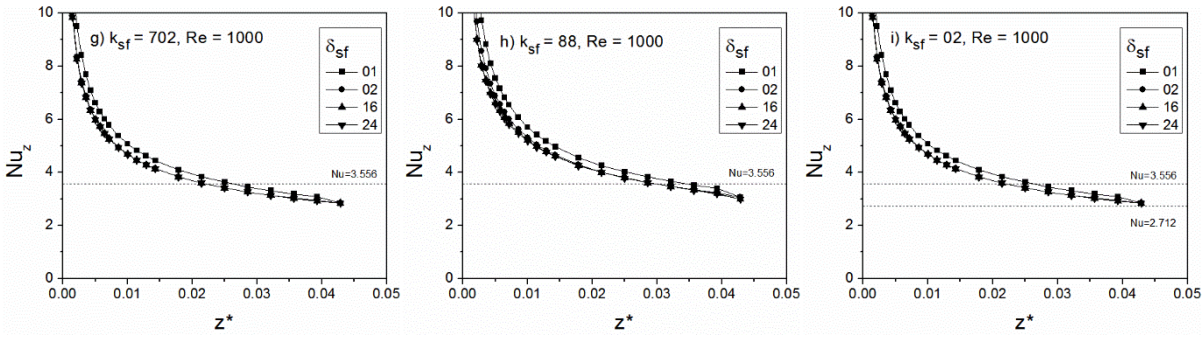

Figure 9: Axial variation of Nu_z in diverging microchannel

The ideal Nusselt number values for zero wall thicknesses are shown in Table 1 with the corresponding boundary condition.

Table 6: Ideal fully developed Nu values with corresponding boundary condition [16]

Sl no	Nu	Boundary condition
1	3.556	Three side heating with one side insulated
2	2.712	One side heating with all other sides insulated

From the plots of Nusselt number with z*, the following observations are made on the dependence of Nusselt number on k_{sf}, δ_{sf} and Re.

1. At higher k_{sf} and δ_{sf} values, the Nu_z values tend to decrease. The reasons for this sensation is same as that of reasons explained in the previous sections of dimensionless heat flux and temperatures.
2. In the middle k_{sf} range, Nusselt number approaches the ideal value of 3.556 which is the situation similar to three side heating. In this case there is very negligible variation of Nu_z with the variation in δ_{sf}. As the k_{sf} values are decreased, the Nusselt number values are increasing up to a certain limiting k_{sf} value.
3. At very low k_{sf} values, the spatial distribution of heat flux applied at the bottom takes place. This makes the situation similar to that of one side wall heating and hence, the value approaches 2.712.

4.2 Inference

From the observations made from Figs. 7-9, it is evident that k_{sf} is a key factor affecting the extent of axial back conduction. So, the variation of average Nusselt number with varying k_{sf} for different Reynolds numbers and δ_{sf} values are presented in Fig. 10 as shown below.

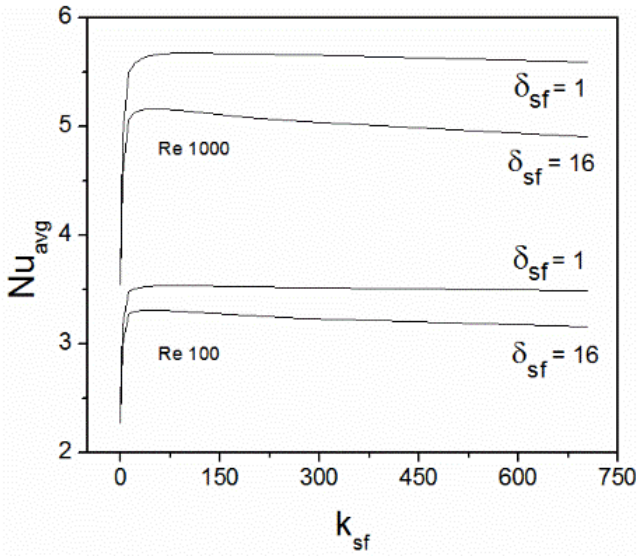

Figure 10: Average Nusselt number of the diverging microchannel versus conductivity ratio (k_{sf}); flow condition (Re) and the thickness ratio (δ_{sf})

Combining all the observations, the following important inferences are made:

1. There exists an optimum value of k_{sf} for which the Nu_z values get maximized.
2. There is a slight decrease of Nu_z with δ_{sf}, especially at higher k_{sf} values.
3. At higher Reynolds number, Nu_z values increases.
4. There is a direct implication of strong and weak functions in determining the effect of axial back conduction. k_{sf} is a strong function and δ_{sf} is a very weak function in affecting the dominance of axial wall conduction.

4.3 Comparison

For the objective of comparison of effect of axial wall conduction in uniform cross sectional microchannels and diverging microchannels, the following plots are made.

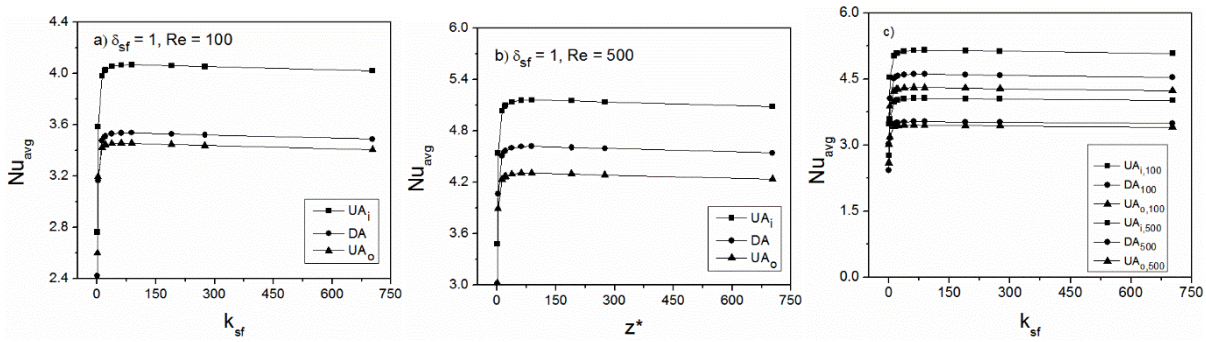

Figure 11: Average Nusselt number of uniform and diverging microchannels at a) δ_{sf} = 1 and Re = 100 and b) δ_{sf} = 1 and Re = 500 c) varying δ_{sf} and Re

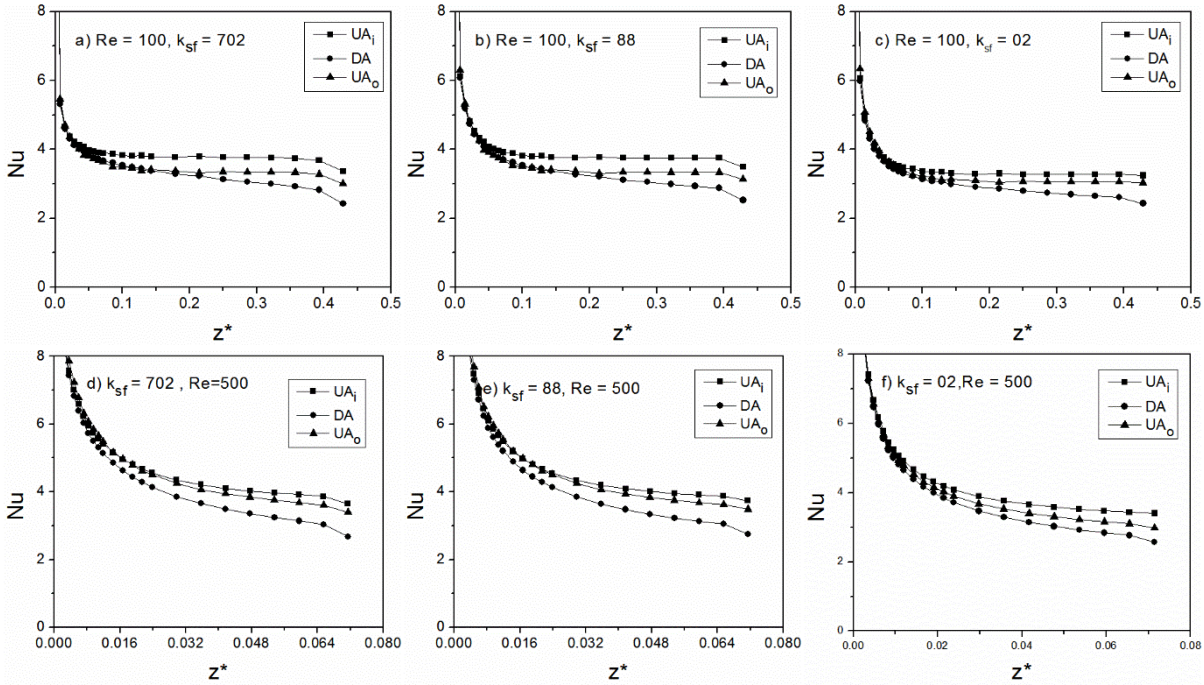

Figure 12 : Plots of Nu_z as a function of dimensionless axial distance at different k_{sf} and Re values

As expected, the diverging Nu_z plots lie in between Nu_z curves of uniform cross sections. For the same k_{sf} value, $Nu_{inlet} > Nu_{diverging\ channel} > Nu_{outlet}$. Here, Nu_{inlet} represents average Nusselt number of uniform cross-sectional microchannel with the cross-sectional dimension equal to that of inlet of diverging microchannel, $Nu_{diverging\ channel}$ represents average Nusselt number of diverging microchannel and Nu_{outlet} represents average Nusselt number of uniform cross-sectional microchannel with the cross-sectional dimension equal to that of inlet of diverging microchannel. Since, the inlet has lesser cross-sectional area, the velocity value in case of uniform microchannel w.r.t inlet is high as compared to that of uniform microchannel w.r.t

outlet. At higher velocities, there is less chance of axial back conduction. This is the possible reason for the outcome trends in this case.

CHAPTER 5

CONCLUSION

To understand and highlight the effects of axial back conduction in case of a diverging rectangular sectional microchannel under simultaneously developing laminar flow and heat transfer, numerical analysis has been carried out on diverging micochannel with constant heat flux condition imposed on the bottom wall of the substrate. A wide parametric variation has been done by varying (k_{sf}~0.33-702); (δ_{sf}~1-24) and (Re~100-1000). The following conclusions have been drawn from the study:

1. k_{sf} is an important parameter affecting the conjugate nature of the present problem. At high k_{sf} values, the average Nusselt number decreases due to the decrease in axial thermal resistance offered by the solid domain.
2. Also, at very low k_{sf} values, the average Nusselt number decreases. A very low k_{sf} value situation is similar to that of situation with zero wall thickness with only one side heated and all other walls kept adiabatic.
3. There exists an optimum value of k_{sf} between the two asymptotes at which the average Nusselt number gets maximized.
4. It is also concluded that similar situation arises for uniform rectangular cross-sectional microchannels. The behavior of diverging microchannels lies in between these uniform microchannels.

REFERENCES

[1] Peterson R. B., "Numerical modeling of conduction effects in microscale counter flow heat exchangers," Journal of Microscale Thermophysics Engineering 3(1), pp. 17-30, 1999.

[2] Bahnke G. D., and Howard C. P., "The effect of longitudinal heat conduction on periodic-flow heat exchanger performance," Journal of Engineering Power 86 (2), pp. 105-120, 1964.

[3] Davis E. J., and Gill N. W., "The effect of axial conduction in the wall on heat transfer with laminar flow," International Journal of Heat and Mass Transfer 13 (3), pp. 459–470, 1970.

[4] Petukhov B. S., "Heat transfer and drag of laminar flow of liquid in pipes," Energiya, Moscow, 1967.

[5] Faghri M., and Sparrow E. M., "Simultaneous wall and fluid axial conduction in laminar pipe-flow heat transfer," Journal of Heat Transfer102(1), pp. 58–63.

[6] Cotton M. A., and Jackson J. D., "The effect of heat conduction in a tube wall upon forced convection heat transfer in the thermal entry region," Journal of Numerical Methods in Thermal Problems T, Pineridge Press, Swansea, vol. Vol. IV, pp. 504–515, 1985.

[7] Chiou J. P., Shah R. K. C., and McDonal C. C. F., "The advancement of compact heat exchanger theory considering the effects of longitudinal heat conduction and flow nonuniformity," ASME-HTD Symposium on Compact Heat Exchangers, vol. Vol. 10, 1980.

[8] Maranzana G., Perry I., and Maillet D., "Mini- and micro-channels: influence of axial conduction in the walls," International Journal of Heat and Mass Transfer, 47(17–18), pp. 3993–4004, 2004.

[9] Zhang S. X., He Y. L., Lauriat G., and Tao W., "Numerical studies of simultaneously developing laminar flow and heat transfer in microtubes with thick wall and constant outside wall temperature," International Journal of Heat and Mass Transfer, 53(19–20), 2010.

[10] Li Z., He Y. L., Tao W. Q., and Tang G. H., "Experimental and numerical studies of liquid flow and heat transfer in microtubes," International Journal of Heat and Mass Transfer, 50(17–18), pp. 3447–3460, 2007.

[11] Toh K. C., Chen X. Y., and Chai J. C., "Numerical computation of fluid flow and heat transfer in micro channels," International Journal of Heat and Mass Transfer, 45(26), pp. 5133 -5141, 2002.

[12] Tiselj I., Hetsroni G., Mavko B., Mosyak A., and Pogre, "Effect of axial conduction on the heat transfer in micro-channels," International Journal of Heat and Mass Transfer 47, pp. 2551–2565, 2004.

[13] Celata G. P., Cumo M., Marconi V., McPhail S. J., "Microtube liquid single phase heat transfer in laminar flow," International Journal of Heat and Mass Transfer, 49(19–20), pp. 3538–3546, 2006.

[14] Tuckerman D. B., and Pease R. F. W., "High-performance heat sinking for VLSI," IEEE Electron Device Letters, 2(5), pp. 126–129, 1981.

[15] Moharana M. K., Agarwal G., and Khandekar S., "Axial conduction in single-phase simultaneously developing flow in a rectangular mini-channel array," International Journal of Thermal Science, 50(6), pp. 1001–1012, 2011.

[16] Moharana M. K., Singh P. K., and Khandekar S., "Optimum Nusselt number for simultaneously developing internal flow under conjugate conditions in a square microchannel," Journal of Heat and Mass Transfer, (134) 071703, pp. 01-10, 2012.

[17] Moharana M. K., and Khandekar S., "Effect of aspect ratio of rectangular microchannels on the axial back conduction in its solid substrate," International Journal of Microscale and Nanoscale Thermal and Fluid Transport Phenomena, vol. IV, no. 3-4, pp. 211-229, 2013.

[18] Moharana M. K., and Khandekar S., "Numerical study of axial back conduction in microtubes," in Thirty Ninth National Conference on Fluid Mechanics, Published by Fluid Power and National Society of Fluid Mechanics & Fluid Power, 2012.

[19] Moharana M. K., and Mishra P., "Axial wall conduction in pulsating laminar flow in a microtube," in 12th International Conference on Nanochannels, Microchannels, and Minichannels, Published by ASME, Chicago, USA, 2014.

[20] Moharana M. K., Singh P. K., and Khandekar S., "Axial heat conduction in the context of developing flows in microchannels," in 9th International Conference on Nanochannels, Microchannels, and Minichannels, Alberta, CANADA, 2011.

[21] Kumar M., and Moharana M. K., "Axial wall conduction in partially heated microtubes," in 22th National and 11th International ISHMT-ASME Heat and Mass Transfer Conference, Published by Indian Society for Heat and Mass Transfer, 2013.

[22] Yadav A., Tiwari N., Moharana M. K., and Sarangi S. K., "Axial wall conduction in cryogenic fluid microtube," 5th International and 41st National Conference on Fluid Mechanics and Fluid Power (FMFP-2014) 12-14 December 2014, IIT Kanpur, India